



HAL
open science

The speed of vaccination rollout and the risk of pathogen adaptation

Sylvain Gandon, Amaury Lambert, Troy Day, Todd L Parsons

► **To cite this version:**

Sylvain Gandon, Amaury Lambert, Troy Day, Todd L Parsons. The speed of vaccination rollout and the risk of pathogen adaptation. 2022. hal-03849469

HAL Id: hal-03849469

<https://cnrs.hal.science/hal-03849469v1>

Preprint submitted on 11 Nov 2022

HAL is a multi-disciplinary open access archive for the deposit and dissemination of scientific research documents, whether they are published or not. The documents may come from teaching and research institutions in France or abroad, or from public or private research centers.

L'archive ouverte pluridisciplinaire **HAL**, est destinée au dépôt et à la diffusion de documents scientifiques de niveau recherche, publiés ou non, émanant des établissements d'enseignement et de recherche français ou étrangers, des laboratoires publics ou privés.

The speed of vaccination rollout and the risk of pathogen adaptation

Sylvain Gandon^{1,*}, Amaury Lambert^{2,3}, Troy Day^{4,5}, and Todd L. Parsons⁶

¹CEFE, CNRS, Univ Montpellier, EPHE, IRD, Montpellier, France

*Corresponding author

²Institut de Biologie de l'ENS (IBENS), École Normale Supérieure (ENS), CNRS UMR 8197, Paris, France

³Center for Interdisciplinary Research in Biology (CIRB), Collège de France, CNRS UMR 7241, INSERM U1050, PSL Research University, Paris, France

⁴Department of Mathematics and Statistics, Queen's University, Kingston, Canada

⁵Department of Biology, Queen's University, Kingston, Canada

⁶Laboratoire de Probabilités, Statistique et Modélisation (LPSM), Sorbonne Université, CNRS UMR 8001, Paris, France

Saturday 13th August, 2022

E-mails: SG - sylvain.gandon@cefe.cnrs.fr; AL - amaury.lambert@ens.fr; TD - tday@mast.queensu.ca; TLP - todd.parsons@upmc.fr;

Keywords: evolutionary epidemiology, vaccination, life-history evolution, demographic stochasticity, virulence, adaptive dynamics

Abstract

Vaccination is expected to reduce disease prevalence and to halt the spread of epidemics. But pathogen adaptation may erode the efficacy of vaccination and challenge our ability to control disease spread. Here we examine the influence of the speed of vaccination rollout on the overall risk of pathogen adaptation to vaccination. We extend the framework of evolutionary epidemiology theory to account for the different steps leading to adaptation to vaccines: (1) introduction of a vaccine-escape variant by mutation from an endemic wild-type pathogen, (2) invasion of this vaccine-escape variant in spite of the risk of early extinction, (3) spread and, eventually, fixation of the vaccine-escape variant in the pathogen population. We show that the risk of pathogen adaptation is maximal for intermediate speed of vaccination rollout. On the one hand, slower rollout decreases pathogen adaptation because selection is too weak to avoid early extinction of the new variant. On the other hand, faster rollout decreases pathogen adaptation because it reduces the influx of adaptive mutations. Hence, vaccinating faster is recommended to decrease both the number of cases and the likelihood of pathogen adaptation. We also show that pathogen adaptation is driven by its basic reproduction ratio, the efficacy of the vaccine and the effects of the vaccine-escape mutations on pathogen life-history traits. Accounting for the interplay between epidemiology, selection and genetic drift, our work clarifies the influence of vaccination policies on different steps of pathogen adaptation and allows us to anticipate the effects of public-health interventions on pathogen evolution.

Significance statement: Pathogen adaptation to host immunity challenges the efficacy of vaccination against infectious diseases. Are there vaccination strategies that limit the emergence and the spread of vaccine-escape variants? Our theoretical model clarifies the interplay between the timing of vaccine escape mutation events and the transient epidemiological dynamics following the start of a vaccination campaign on pathogen adaptation. We show that the risk of adaptation is maximized for intermediate vaccination coverage but can be reduced by a combination of non pharmaceutical interventions and maximizing the speed of the vaccination rollout. These recommendations may have important implications for the choice of vaccination strategies against the ongoing SARS-CoV-2 pandemic.

21 1 Introduction

22 Vaccination offers unique opportunities to protect a large fraction of the host population and
23 thus to control spreading epidemics. In principle, large vaccination coverage can lead to pathogen
24 eradication. In practice, however, the coverage required for eradication is often impossible to
25 reach with imperfect vaccines [16, 34]. Moreover, pathogen adaptation may erode the efficacy of
26 vaccination. Even if adaptation to vaccines is less common than adaptation to drugs [14, 25, 26]
27 the spread of vaccine-escape mutations may challenge our ability to halt the spread of epidemics.

28 Understanding the dynamics of pathogen adaptation to vaccines is particularly relevant in the
29 control of the ongoing SARS-CoV-2 pandemic. Yet, most theoretical studies that explore the
30 evolution of pathogens after vaccination are based on the analysis of deterministic models and
31 ignore the potential effects induced by the stochasticity of epidemiological dynamics. Demographic
32 stochasticity, however, drives the intensity of genetic drift and can affect the establishment of new
33 mutations and the long-term evolution of pathogens [42, 44, 41]. Several studies showed how the
34 demographic stochasticity induced by finite host and pathogen population sizes alters selection on
35 the life-history traits of pathogens [28, 22, 36]. These analytical predictions rely on the assumption
36 that mutation rate is low, which allows us to decouple epidemiological and evolutionary time scales.
37 Indeed, when mutation rate is low, the new strain is always introduced after the resident pathogen
38 population has reached its endemic equilibrium. Many pathogens, however, have relatively large
39 mutation rates [43] and the fate of a pathogen mutant introduced away from the endemic equilibrium
40 is likely to be affected by the dynamics of the pathogen populations. Besides, the start of a
41 vaccination campaign is expected to yield massive perturbations of the epidemiological dynamics
42 and new mutations are likely to appear when the pathogen population is far from its endemic
43 equilibrium.

44 The aim of the present study is to develop a versatile theoretical framework to evaluate the
45 consequences of vaccination on the risk of pathogen adaptation to vaccination. There are six
46 main evolutionary epidemiology outcomes after the start of vaccination which are summarized in
47 **Figure 1**. Some of these outcomes are more favorable than others because they do not lead to
48 the invasion of a new variant (**Figure 1a-c**). In contrast, vaccination may lead to the invasion of

49 vaccine-escape variants (**Figure 1e-f**). In the following we use a combination of deterministic and
50 branching process approximations to study the joint epidemiological and evolutionary dynamics
51 of the pathogen population. This analysis reveals the importance of the speed of the vaccination
52 rollout as well as of the life-history characteristics of the vaccine-escape variants on the probability
53 of pathogen adaptation.

54 2 Model

55 We use a classical SIR epidemiological model with demography, where hosts can either be suscepti-
56 ble, infected or recovered [3]. The discrete number of each of these types of hosts is denoted by S^n ,
57 I^n and R^n , respectively. Because we are interested in the effect of demographic stochasticity the
58 model is derived from a microscopic description of all the events that may occur in a finite—but not
59 fixed—host population of (varying) total size $N^n = S^n + I^n + R^n$. We consider a continuous-time
60 Markov process tracking the number of individuals of each type of host (see SI Section 1 for a
61 detailed description). The susceptible hosts immigrate at rate λn , where n is a “system size”, or
62 scaling parameter, that indicates the order of magnitude of the arena in which the epidemic occurs.
63 Hence the total host population varies stochastically in time, but remains of the order of n .

64 Vaccination may either take place with probability p when a new susceptible host enters the
65 population (e.g., vaccination of newborns) or at a constant rate ν for all other susceptible hosts
66 (e.g., vaccination of adults). The immunity triggered by vaccination is assumed to wane at rate
67 ω . A host may be unvaccinated, U , or vaccinated, V , and may either be uninfected or infected
68 with the wild type, w , or a mutant strain, m (we assume coinfections are not possible). We thus
69 have to track the numbers of two classes of susceptible hosts (S_U^n, S_V^n) and four classes of infected
70 individuals ($I_{Uw}^n, I_{Um}^n, I_{Vw}^n, I_{Vm}^n$). We assume that the virulence α_i (the mortality rate induced by
71 the infection), the transmission β_i (the production rate of new infections), and the recovery γ_i (the
72 rate at which the host clears the infection) are fully governed by the pathogen genotype ($i = w$ or
73 m). A fourth trait $e_i \in [0, 1]$ governs the infectivity of pathogen genotype i on vaccinated hosts
74 (infectivity of all genotypes is assumed to be equal to 1 on unvaccinated hosts). In other words, this
75 final trait measures the ability of the pathogen to escape the immunity triggered by the vaccine.

76 For simplicity we assume that recovered hosts have lifelong immunity and thus reinfection is not
 77 possible. We assume frequency-dependent transmission where the number of contacts a host may
 78 have in the population is constant but a proportion of those contacts may be infectious. Note,
 79 however, that other forms of transmission (e.g. density-dependent transmission [33]) are expected
 80 to yield qualitatively similar results. We summarize the states of the process and the jump rates
 81 at which individuals transition between states in **Table S1** and in **Figure 2**.

82 We use this model to examine the epidemiological and evolutionary dynamics following the
 83 start of the vaccination campaign. In the following, for the sake of simplicity, we focus on scenarios
 84 where we assume the pathogen population has reached an endemic equilibrium before the start of
 85 vaccination (but we consider alternative scenarios in the Discussion).

86 3 Results

87 3.1 Deterministic Approximation

88 As a first step in our analysis, we use a deterministic approximation for large values of n [29] and
 89 we work with host densities defined as $S_i = S_i^n/n$, $I_{ij} = I_{ij}^n/n$, $N = N^n/n$. This corresponds
 90 to replacing discrete individuals by densities and interpreting the rates in **Figure 2** as describing
 91 continuous flows rather than jumps. This yields a system of ordinary differential equations:

$$\begin{aligned}
 \dot{S}_U &= \lambda(1-p) + \omega S_V - \left(\beta_w \frac{I_{Uw} + I_{Vw}}{N} + \beta_m \frac{I_{Um} + I_{Vm}}{N} + \delta + \nu \right) S_U \\
 \dot{S}_V &= \lambda p + \nu S_U - \left(e_w \beta_w \frac{I_{Uw} + I_{Vw}}{N} + e_m \beta_m \frac{I_{Um} + I_{Vm}}{N} + \delta + \omega \right) S_V \\
 \dot{I}_{Uw} &= \beta_w (I_{Uw} + I_{Vw}) \frac{S_U}{N} - (\delta + \alpha_w + \gamma_w) I_{Uw} \\
 \dot{I}_{Um} &= \beta_m (I_{Um} + I_{Vm}) \frac{S_U}{N} - (\delta + \alpha_m + \gamma_m) I_{Um} \\
 \dot{I}_{Vw} &= e_w \beta_w (I_{Uw} + I_{Vw}) \frac{S_V}{N} - (\delta + \alpha_w + \gamma_w) I_{Vw} \\
 \dot{I}_{Vm} &= e_m \beta_m (I_{Um} + I_{Vm}) \frac{S_V}{N} - (\delta + \alpha_m + \gamma_m) I_{Vm} \\
 \dot{N} &= \lambda - \delta N - \alpha_w (I_{Uw} + I_{Vw}) - \alpha_m (I_{Um} + I_{Vm}),
 \end{aligned} \tag{1}$$

92

93 It is also convenient to track the dynamics of the total density of hosts infected with the same
 94 strain i , $I_i := I_{U_i} + I_{V_i}$, which yields:

$$\dot{I}_i = \underbrace{\left(\left(\beta_i \frac{S_U}{N} + e_i \beta_i \frac{S_V}{N} \right) - (\delta + \alpha_i + \gamma_i) \right)}_{r_i = \text{growth rate of strain } i} I_i \quad (2)$$

95 The ability of the strains to grow is given by the sign of the growth rate r_i . Note that this growth
 96 rate depends on the four different traits of the pathogen: $\alpha_i, \beta_i, \gamma_i, e_i$. But this growth rate depends
 97 also on the densities S_U and S_V , which vary with t , the time since the start of vaccination (i.e.,
 98 vaccination starts at $t = 0$). The coefficient of selection s_m on the mutant strain relative to the
 99 wild type is:

$$s_m = r_m - r_w = (\beta_m - \beta_w) \frac{S_U}{N} + (e_m \beta_m - e_w \beta_w) \frac{S_V}{N} - (\alpha_m - \alpha_w + \gamma_m - \gamma_w) \quad (3)$$

100 In other words, both the genetics (the traits of strain i) and the environment (the epidemiological
 101 state of the host population) govern selection and strain dynamics.

102 3.2 Pathogen eradication and vaccination threshold

103 The ability of the wild-type pathogen population to grow can be measured by its effective per-
 104 generation reproduction ratio which is given by:

$$R_w^e = R_w \left(\frac{S_U}{N} + e_i \frac{S_V}{N} \right) \quad (4)$$

105 where $R_i = \frac{\beta_i}{\delta + \alpha_i + \gamma_i}$. Hence, a reduction of the availability of susceptible hosts with vaccination
 106 may drive down the density of the wild-type pathogen when the production of new infected hosts
 107 (infection “birth”) does not compensate for the recovery and death of infected hosts (infection
 108 “death”), that is when $R_w^e < 1$. Ultimately, vaccination can even lead to the eradication of the
 109 wild-type pathogen (**Figure 1a**) either when the vaccine is sufficiently efficient ($e_w R_w > 1$) or
 110 when the vaccination coverage is sufficiently high [34, 16]. The deterministic model (1) can be used

111 to identify the threshold ν_c of the speed of vaccination rollout above which the wild-type pathogen
112 can be driven to extinction (see Methods and SI Section 1):

$$\nu_c = \frac{R_w(\delta(1 - (1 - e_w)p) + \omega) - (\delta + \omega)}{1 - R_w e_w} \quad (5)$$

113 As expected, better vaccines (i.e., lower values of e_w and ω) yield lower threshold values for the
114 speed of vaccination. Imperfect vaccines (i.e., higher values of e_w and ω), in contrast, are un-
115 likely to allow eradication. Note that, if we wait sufficiently long, the population of the wild-type
116 pathogen will be driven to extinction in a *stochastic* way even when $\nu < \nu_c$. Indeed, in a finite
117 host population, sooner or later, the pathogen population is doomed to become extinct because of
118 demographic stochasticity, but the extinction time when $\nu < \nu_c$ will usually be very long, increas-
119 ing exponentially with the system size n . From now on, we are going to neglect the possibility of
120 extinction of the wild type due to vaccination when $\nu < \nu_c$ (which is a good approximation when
121 n is large) but will return to it in the discussion.

122

123 The spread of a new pathogen variant may erode the efficacy of vaccination and, consequently,
124 could affect the ability to control and, ultimately, to eradicate the pathogen. But before the
125 replacement of the wild type by a vaccine-escape variant the pathogen population may go through
126 three steps that may result (or not) in pathogen adaptation: (1) introduction of the vaccine-escape
127 variant by mutation, (2) extinction (**Figure 1c**) or invasion (**Figure 1d-e**) of the vaccine-escape
128 variant, (3) fixation (**Figure 1e**) or not of the vaccine-adapted variant. Each of these steps is very
129 sensitive to stochasticity because the number of vaccine-escape variants is very small in the early
130 phase of its emergence.

131 **3.3 Step 1: Introduction of the variant by mutation**

132 The first step of adaptation is driven by the production of new variants by the wild-type pathogen
133 through mutation. The level of adaptation to unvaccinated and vaccinated hosts may vary among
134 those variants [10]. Vaccine-escape mutations that do not carry any fitness costs (or may even
135 be adaptive) in unvaccinated hosts are expected to invade and fix relatively easily irrespective of

136 the vaccination strategy. We thus focus on variants that carry fitness costs in immunologically
137 naïve hosts (i.e., variants *specialized* on vaccinated hosts [10]). In principle, the introduction of
138 the vaccine-escape mutation may occur before the rollout of vaccination. The distribution of these
139 mutations is expected to follow a stationary distribution resulting from the action of recurrent
140 mutations and negative selection (see Methods). If these fitness costs are high and/or if the mutation
141 rate is low these pre-existing mutants are expected to be rare. In the following, we neglect the
142 presence or pre-existing mutants and we focus on a scenario where the first vaccine-escape mutant
143 appears after the start of vaccination (but see Methods, section 5.5).

144 At the onset of the vaccination campaign (i.e., $t = 0$) we assume that the system is at the
145 endemic equilibrium (i.e., the equilibrium densities S_U^0 , I_{Uw}^0 and I_{Vw}^0 are given in (11) in the
146 Methods). We assume that an individual host infected with the wild type produces vaccine-escape
147 mutants at a small, constant rate θ_U/n if unvaccinated and θ_V/n if vaccinated. In addition, we
148 assume that θ_U and θ_V are small enough that within-host clonal interference is unlikely, and that
149 $\theta_V \geq \theta_U$ to account for the fact that within-host selection may favor mutants in vaccinated hosts.
150 The total production of mutants is thus equal to $\frac{\theta_U}{n} I_{Uw}^n(t) + \frac{\theta_V}{n} I_{Vw}^n(t) \approx \theta_U I_{Uw}(t) + \theta_V I_{Vw}(t)$,
151 so that the probability density $f_m(t)$ of the arrival time $t = t_m$ of the vaccine-escape mutant is
152 approximated by:

$$f_m(t) = (\theta_U I_{Uw}(t) + \theta_V I_{Vw}(t)) e^{-\int_0^t (\theta_U I_{Uw}(s) + \theta_V I_{Vw}(s)) ds}. \quad (6)$$

153 In other words, the time t_m at which the vaccine-escape variant is introduced by mutation
154 depends on the dynamics of the incidence of the infections by the wild type. Plots of f_m for
155 different values of rollout speed ν in **Figure 3** show that a faster rollout of vaccination delays the
156 introduction of the vaccine-escape mutant. Indeed, a faster rollout is known to result in a drop
157 of the incidence (the honey-moon period) [34, 13] which is expected to decrease the influx of new
158 variants during this period. **Figure 3** also shows how higher values of θ_V can increase the influx of
159 vaccine-escape variants. As discussed in the following section, the subsequent fate of vaccine-escape
160 mutants depends strongly on the timing of their arrival.

161 3.4 Step 2: Variant invasion

162 Immediately after its introduction, the dynamics of the vaccine-escape mutant may be approximated
163 by a time-inhomogeneous birth-death process where the rate of birth (i.e., rate of new infections
164 by the mutant) varies with the availability of susceptible hosts (see Methods, section 5.3). The
165 probability that a single mutant with time-varying birth rate $b_m(t) = \beta_m \left(\frac{S_U(t)}{N(t)} + \frac{e_m S_V(t)}{N(t)} \right)$ and
166 constant death rate $d_m = \delta + \alpha_m + \gamma_m$, introduced at time t_m , successfully invades (see [24] and
167 SI, Section 2) is:

$$P_m^{t_m} = \frac{1}{1 + \int_{t_m}^{\infty} d_m e^{-\int_{t_m}^t b_m(s) - d_m ds} dt} \quad (7)$$

168 Plotting the probability of invasion vs. t_m in **Figure 4** shows that the time at which the vaccine-
169 escape mutant is introduced has a dramatic impact on the probability of escaping early extinction.
170 If the mutant is introduced early, the density $S_V(t)$ of susceptible vaccinated hosts remains very
171 low and the selection for the vaccine-escape mutant is too small to prevent stochastic extinctions.
172 The probability of invasion increases with selection, and thus with the density of vaccinated hosts,
173 which tends to increase with time (see equation (3)).

174 Taking $t_m \rightarrow \infty$ allows us to tackle the situation when the vaccine-escape mutant appears at
175 the endemic equilibrium, i.e., when the densities of unvaccinated and vaccinated susceptible hosts
176 are S_U^* and S_V^* , respectively. At that point in time the effective per-generation reproduction ratio
177 of genotype i (i.e. the expected number of secondary infections produced by pathogen genotype i)
178 is:

$$R_i^* = R_i \left(\frac{S_U^*}{N^*} + e_i \frac{S_V^*}{N^*} \right) \quad (8)$$

179 By definition, at the endemic equilibrium set by the wild-type pathogen we have $R_w^* = R_w^e = 1$.
180 Hence, a necessary condition for the mutant to invade this equilibrium is $R_m^* > 1$, i.e., the effective
181 reproduction number of the mutant has to be higher than that of the wild type (see SI, Section 1).
182 However, this is not a sufficient condition: many mutants that satisfy this condition will rapidly
183 go extinct due to demographic stochasticity. But in contrast to an early introduction of the mu-
184 tant discussed above, the stochastic dynamics of the mutant is approximately a *time-homogeneous*
185 branching process because the birth rate of the mutant approaches $b_m^* = \beta_i \left(\frac{S_U^*}{N^*} + e_i \frac{S_V^*}{N^*} \right)$. This

186 birth rate is constant because the density of susceptible hosts remains constant at the endemic
187 equilibrium. The probability of mutant invasion after introducing a single host infected by the
188 mutant is thus (see SI Section 1; **Figure 4**):

$$P_m^* = \lim_{t_m \rightarrow \infty} P_m^{t_m} = 1 - \frac{R_w^*}{R_m^*} = 1 - \frac{1}{R_m^*} \quad (9)$$

189 Note that we recover the strong-selection result of [36]. This expression shows that *at this endemic*
190 *equilibrium* the fate of the mutant is fully governed by the per-generation reproduction ratio of
191 the two strains, but does not depend on the specific values of the life-history traits of the mutant
192 (provided the different vaccine-escape variants have the same value of R_m^*).

193 Interestingly, unlike P_m^* , the probability $P_m^{t_m}$ of mutant invasion at time t_m given in (7) is not
194 governed solely by R_i , but rather depends on the life-history traits of the mutants. For instance,
195 assume that two vaccine-escape mutants have the same values of R_m and e_m but they have very
196 different life-history strategies. The “slow” strain has low rates of transmission and virulence (in
197 green in **Figure 4**) while the “fast” strain has high rates of transmission and virulence (in red
198 in **Figure 4**). **Figure 4** shows that the high mortality rate of hosts infected by the fast strain
199 increases the risk of early extinction and lowers the probability of invasion relative to the slow
200 strain. Hence, in the early stage of adaptation, pathogen life-history matters and favours slow
201 strains with lower rates of transmission and virulence.

202 **3.5 Step 3: After variant invasion**

203 Successful invasion of the vaccine-escape mutant means that it escaped the “danger zone” when its
204 density is so low that it is very likely to go extinct (**Figure 1d-f**). After this invasion we can describe
205 the dynamics of the polymorphic pathogen population using the deterministic approximation (1).

206 Because the invasion of the mutant at the endemic equilibrium set by the wild type requires
207 that $R_m^* > R_w^*$, we may expect from the analysis of the deterministic model that the mutant would
208 always replace the wild-type pathogen. That is, the wild-type pathogen would go extinct before
209 the mutant (**Figure 1f**). This is indeed the case when the phenotypes of the mutant and the wild
210 type are not very different because of the “invasion implies fixation” principle [17, 5, 38]. Yet, this

211 principle may be violated if the phenotype of the vaccine-escape mutant is very different than the
212 phenotype of the wild type.

213 First, if the two genotypes (w and m) are sufficiently specialized on the two hosts, the long-term
214 coexistence of the two genotypes is possible (**Figure 1e**). Second, the vaccine-escape mutant may
215 be driven to extinction before the wild type if its life-history traits induce massive epidemiological
216 perturbations after its successful invasion (**Figure 1d**). As pointed out by previous studies, more
217 transmissible and aggressive pathogen strategies may yield larger epidemics because the speed of
218 the epidemic is governed by the per-capita growth rate r_i , not the per-generation reproduction
219 ratio R_i [13]. This explosive dynamics is followed by a decline which results in a very low incidence
220 of the vaccine-escape mutant. In a finite host population, this may result in the extinction of the
221 vaccine-escape mutant before the wild type [42]. We capture this outcome with a hybrid analytical-
222 numerical approach that computes the probability $P_{fix}^{t_m}$ that the wild type will go extinct before
223 the mutant (see Methods, section 5.4). **Figure 5** shows that two vaccine-escape mutants may have
224 very different probabilities of fixation, even if they have the same per-generation reproduction ratio.
225 The numerical computation of the probability of fixation agrees very well with individual-based
226 stochastic simulations (**Figure S1**). The faster strain is unlikely to go to fixation because invasion
227 is followed by a period where the birth rate drops to very low levels (far below the mortality
228 rates, **Figure S2**). In other words, a more aggressive strategy will more rapidly degrade its
229 environment, by depleting susceptible hosts, which is known to increase the probability of extinction
230 [6]. Interestingly, this effect is only apparent when the time of introduction t_m is large. Indeed,
231 when the mutant is introduced soon after the start of vaccination, its probability of invasion is
232 already very low because its initial growth rate is negative (**Figure S2a, b, c**). When the mutant
233 is introduced at intermediate times, the initial growth rate of the mutant is positive because some
234 hosts are vaccinated (**Figure S2d, e, f**). If the vaccine-escape mutant is introduced later, the
235 growth rate of the mutant is initially very high as many hosts are vaccinated (and thus susceptible
236 to the vaccine-escape mutant) but this is rapidly followed by a drop in host density (especially
237 pronounced with the faster strain) which prevents the long-term establishment of the faster strain
238 (see **Figure S2g, h, i**).

239 3.6 The overall risk of pathogen adaptation

240 The overall probability that the pathogen will adapt to vaccination (*i.e.* that a vaccine-escape
241 variant will replace the wild-type) depends upon the probability that the mutation will arise (step
242 1) and the probability that this mutation will escape early extinction (step 2) and eventually go to
243 fixation (step 3). It is particularly relevant to explore the effect of the speed of vaccination rollout
244 on the overall probability that some vaccine-adapted variant invades before a time t after the start
245 of the vaccination campaign (steps 1 and 2, **Figure 6**):

$$A_m^t = 1 - e^{-\int_0^t (\theta_U I_{Uw}(s) + \theta_V I_{Vw}(s)) P_m^s ds}. \quad (10)$$

246 As expected, when $\nu < \nu_c$ this probability of adaptation goes to 1 when $t \rightarrow \infty$. Indeed,
247 when vaccination cannot eradicate the wild type, a vaccine-adapted variant will eventually appear
248 by mutation and invade. When $\nu > \nu_c$, we recover a classical evolutionary rescue scenario where
249 the arrival and the spread of a vaccine-adapted variant may stop the eradication [32, 2, 4]. Since
250 vaccination is unlikely to lead to eradication we focus here on a scenario where $\nu < \nu_c$ and we
251 use equation (10) to analyse the effect of the speed of adaptation on the probability of pathogen
252 adaptation at a time t after the start of vaccination. Crucially, the risk of pathogen adaptation is
253 maximized for intermediate values of the speed of vaccination rollout. This is due to the antagonistic
254 consequences the speed of the rollout has upon these two steps of adaptation (compare **Figures 3**
255 **and 4**). Faster rollout reduces the influx of new mutations, but increases selection for vaccine-escape
256 mutations. Notice how the risk of adaptation drops with the speed of the rollout of vaccination
257 before the critical speed, $\nu < \nu_c$, that may ultimately lead to eradication. When the speed of
258 vaccination is just below ν_c , vaccination coverage is not high enough to allow eradication, but it is
259 high enough to reduce massively the probability of adaptation through the reduction of the influx of
260 new mutations. As expected, variants with different life-history may have different probabilities of
261 adaptation. Indeed, as pointed out in the previous section, faster variants have a lower probability
262 of invasion when the variant is introduced at the beginning of the vaccination campaign (**Figure**
263 **4**). This effect is relatively small but it is expected to be magnified by the subsequent risk of

264 extinction following invasion (**Figure 5**).

265 4 Discussion

266 Vaccination is a powerful tool to control the spread of infectious diseases, but some pathogens
267 evolve to escape the immunity triggered by vaccines. Will SARS-CoV-2 continue to adapt to the
268 different vaccines that are currently being used to halt the ongoing pandemic? Does the likelihood
269 of this adaptation depend on the speed of the vaccination rollout? To answer these questions we
270 must first understand the different steps that may eventually lead to adaptation to vaccination.

271 Mutation is the fuel of evolution, and the first step of adaptation to vaccination is the mutational
272 process that produces vaccine-escape variants. Even if initial estimates of SARS-CoV-2 mutation
273 rates were reassuringly low [39], the virus has managed to evolve higher rates of transmission [9, 46]
274 and these adaptations are challenging current control measures used to slow down the ongoing
275 pandemic. The ability of the new variants of SARS-CoV-2 to escape immunity is also worrying
276 and indicates that viral adaption can weaken vaccine efficacy [47, 37]. The rate at which these
277 potential vaccine-escape mutations are introduced depends on the density of hosts infected by the
278 wild-type virus. In this respect, a faster rollout of vaccination is expected to delay the arrival of
279 these mutations (**Figure 3**).

280 Some authors have argued that the emergence of vaccine-escape mutations may be more likely
281 in infected hosts which are partially immunized [12, 8, 10]. Our model can be used to explore
282 the consequences of this within-host evolution in vaccinated hosts (*e.g.*, taking $\theta_V > \theta_U$). A
283 larger value of θ_V increases the overall rate of mutation (**Figure 3**) but this effect is modulated
284 by the fraction of the host population that is vaccinated. Consequently, when $\theta_V > \theta_U$, the
285 speed of vaccination rollout can have a non-monotonic effect on the probability that a vaccine-
286 escape mutation is introduced (see **Figure S3**). Indeed, when the rate of vaccination remains low,
287 the enhancing effect of vaccination on the rate of mutation can counteract the delaying effect of
288 faster vaccination rollout discussed above. But the probability that a vaccine-escape mutation is
289 introduced drops to very low levels when the rate of vaccination becomes overwhelmingly high.

290 The second step of adaptation starts as soon as the vaccine-escape mutant has been introduced

291 in the pathogen population. Will this new variant go extinct rapidly or will it start to invade? The
292 answer to this question depends on the time at which the mutant is introduced. If the mutant is
293 introduced when the population is not at an endemic equilibrium, the fate of the mutant depends
294 on a time-varying birth rate which is driven by the fluctuations of the density of susceptible hosts.
295 Earlier introductions are likely to result in rapid extinction because there are simply not enough
296 vaccinated hosts to favour the mutant over the wild type. Moreover, we found that earlier introduc-
297 tions are likely to favour slower life-history strategies which are less prone to early extinction. If the
298 introduction takes place later, when the system has reached a new endemic equilibrium, the fate
299 of the mutant is solely governed by the effective per-generation ratio R_m^* and does not depend on
300 the life-history traits of the mutant. Slow and fast variants have equal probability to invade if they
301 have the same R_m^* . Altogether, our results suggest that earlier arrival may not always facilitate
302 invasion since the probability of invasion is limited by the time-varying epidemiological state of the
303 host population.

304 The third step of adaptation starts as soon as the hosts infected by the vaccine-escape mutant
305 are abundant and the effect of demographic stochasticity on the dynamics of this mutation becomes
306 negligible. Our analysis attempts to better characterize the dynamics of the mutant after invasion
307 using a combination of deterministic and analytical approximations. In principle, conditional on
308 invasion, we can use the deterministic model (1) to describe the joint dynamics of the mutant and
309 the wild type. In particular, the speed at which the vaccine-escape mutant spreads in the pathogen
310 population can be well approximated by the deterministic model. This may be particularly useful to
311 address the impact of various vaccination strategies on the speed of the spread of a vaccine-adapted
312 variant [15]. In the present work we show that life-history traits of the vaccine-escape mutant drive
313 the speed of its spread. Indeed, as pointed out before, the deterministic transient dynamics depends
314 on the per-capita growth rate of the mutant r_m , not its per-generation reproduction ratio R_m [13].
315 Transient dynamics may favour a fast and aggressive variant because this life-history strategy may
316 be more competitive away from the endemic equilibrium. Yet, this explosive strategy may be risky
317 for the pathogen if it leads to epidemiological fluctuations that result in a massive drop in the
318 number of infections. The consequences of such fluctuations on the extinction risk of the variant

319 can be accounted for by a generalized birth-death process where the per-capita growth rate of
320 the mutant varies with time. Epidemiological fluctuations lead to a degradation of the future
321 environment (i.e., depletion of the density of susceptible hosts) which results in an increased risk
322 of extinction [24, 6].

323 A comprehensive understanding of pathogen dynamics after vaccination relies on the use of
324 a combination of theoretical tools to capture the interplay between stochastic and deterministic
325 forces. Here, we use a hybrid numerical-analytical approach to account for the three successive steps
326 that may eventually lead to the fixation of a vaccine-escape mutant. This theoretical framework
327 is particularly suitable to explore the influence of different vaccination strategies on the risk of
328 pathogen adaptation. In particular, we show that this risk drops to very low levels even when the
329 speed of vaccination rollout is below the threshold value that may eventually lead to eradication
330 (i.e., $\nu < \nu_c$). In other words, faster vaccination rollout makes sense even when eradication is
331 infeasible, because faster rollout decreases both the number of cases and the likelihood of pathogen
332 evolution. This conclusion is akin to the general prediction that the rate of pathogen adaptation
333 should be maximized for intermediate immune pressure or for medium doses of chemotherapy at
334 the within-host level [20, 40, 19, 1, 21, 11, 2]. Most of these earlier studies focused on evolutionary
335 rescue scenarios where the wild type is expected to be rapidly driven to extinction by human
336 intervention. Our versatile theoretical framework, however, allows us to deal with a broad range
337 of situations where the intervention is not expected to eradicate the pathogen. Accounting for the
338 dynamics of the wild type affects both the flux of mutation and the fate of these mutations.

339 The framework we have developed can be readily extended to explore many other situations.
340 For instance, our model can be modified to explore the influence of temporal variations in the
341 environment that could be driven by seasonality or by non-pharmaceutical interventions (NPIs).
342 We explored a situation where the transmission rate of all variants is periodically reduced by a
343 quantity $1 - c(t)$, where $c(t)$ is a measure of the intensity of NPIs. These periodic interventions affect
344 both the flux of mutations and the probability that these mutations invade (**Figures S3** and **S4**).
345 Notably, NPIs lower the probability of mutant introduction through the reduction in the density of
346 hosts infected by the wild type. As a consequence, the probability of adaptation is reduced when

347 vaccination is combined with periodic control measures (**Figure 6**). Hence, our approach helps to
348 understand the interaction between vaccination and NPI discussed in earlier studies [41, 31]. An
349 important limitation of this study is that, for conceptual clarity, we have made several simplifying
350 assumptions that would need to be relaxed to confidently apply our findings to the current SARS-
351 CoV-2 pandemic. First, one should study situations where the pathogen population has not reached
352 an endemic equilibrium when selection (e.g., vaccination or chemotherapy) starts to be applied.
353 Second, it would be necessary to relax other assumptions made here, such as frequency-dependent
354 transmission or life-long immunity after recovery. Accounting for natural recovery would require yet
355 another class of imperfectly immune hosts. Similarly, another important extension of our model
356 would be to study the effect of a diversity of vaccines in the host population. This diversity of
357 immune profiles could slow down pathogen adaptation if the escape of different vaccines requires
358 distinct mutations [45, 7, 35]. Finally, it is important to recall that we focus here on a simplified
359 scenario where we analyse the evolutionary epidemiology of an isolated population. In real-life
360 situations the arrival time may depend more on the immigration of new variants from abroad than
361 on local vaccination policies. The influence of migration remains to be investigated in spatially
362 structured models where vaccination may vary among populations [18].

363 5 Methods

364 In this section, we present how extinction, invasion and fixation probabilities may be obtained
365 under strong-selection assumptions when a mutant strain appears in a host-pathogen system that
366 is away from its endemic equilibrium. Our essential tools are the deterministic ordinary differential
367 equations (1) and birth-and-death approximations, which we discuss below. The former allows us to
368 consider the situation when all strains are abundant, the latter when at least one strain is rare. We
369 will limit ourselves to an informal treatment, presenting heuristic arguments and deferring rigorous
370 proofs and sharp error bounds to a future treatment. In the following we present a simple, yet
371 versatile, hybrid (i.e., semi-deterministic) framework which allows us to approximate the probabili-
372 ties associated with different steps of adaptation (mutation, invasion, fixation) via adding auxiliary
373 equations describing stochastic phenomena, to the deterministic ordinary differential equations

374 describing the global population dynamics.

375 5.1 Before the introduction of a variant

376 We assume that vaccination starts after the monomorphic population of the wild-type pathogen
377 has reached its endemic equilibrium,

$$\begin{aligned}
 S_U^0 &= \frac{\lambda(\delta + \gamma_w)}{\delta(\beta_w - \alpha_w)} \\
 S_V^0 &= 0 \\
 I_{Uw}^0 &= \frac{\lambda(R_w - 1)}{\beta_w - \alpha_w} \\
 I_{Vw}^0 &= 0 \\
 N^0 &= \frac{\lambda R_w(\delta + \gamma_w)}{\delta(\beta_w - \alpha_w)}
 \end{aligned} \tag{11}$$

378 We then use the following ordinary differential equations to track the deterministic dynamics
379 of the wild-type pathogen using the endemic equilibrium before vaccination (11) as the initial
380 condition:

$$\begin{aligned}
 \dot{S}_U &= \lambda(1 - p) + \omega S_V - \left(\beta_w \frac{I_{Uw} + I_{Vw}}{N} + \delta + \nu \right) S_U \\
 \dot{S}_V &= \lambda p + \nu S_U - \left(e_w \beta_w \frac{I_{Uw} + I_{Vw}}{N} + \delta + \omega \right) S_V \\
 \dot{I}_{Uw} &= \beta_w (I_{Uw} + I_{Vw}) \frac{S_U}{N} - (\delta + \alpha_w + \gamma_w) I_{Uw} \\
 \dot{I}_{Vw} &= e_w \beta_w (I_{Uw} + I_{Vw}) \frac{S_V}{N} - (\delta + \alpha_w + \gamma_w) I_{Vw} \\
 \dot{N} &= \lambda - \delta N - \alpha_w (I_{Uw} + I_{Vw}).
 \end{aligned} \tag{12}$$

Letting $I_w = I_{Uw} + I_{Vw}$, we get from (12):

$$\dot{I}_w = \beta_w (S_U + e_w S_V) \frac{I_w}{N} - (\delta + \alpha_w + \gamma_w) I_w.$$

A new endemic equilibrium will thus be approached after vaccination if and only if the growth rate $r_w = \beta_w (S_U + e_w S_V) / N - (\delta + \alpha_w + \gamma_w)$ is positive, or equivalently if the effective per-generation

reproduction ratio

$$R_w^e = R_w \left(\frac{S_U}{N} + e_w \frac{S_V}{N} \right)$$

381 is larger than 1, when S_U and S_V are taking their stationary values \tilde{S}_U and \tilde{S}_V in the absence of
382 infection. Computing these values (see SI, Section 1) shows that $R_w^e > 1$ if and only if $e_w R_w > 1$
383 or $\nu > \nu_c$, where

$$\nu_c = \frac{R_w(\delta(1 - (1 - e_w)p) + \omega) - (\delta + \omega)}{1 - R_w e_w} \quad (13)$$

384 Thus we see that if $e_w R_w < 1$ and the speed of the vaccination rollout is higher than the critical
385 value ν_c the wild type will be driven to extinction deterministically.

386 For values of the vaccination rollout ν smaller than this threshold ν_c , or when $e_w R_w > 1$, the wild-
387 type may also become extinct because of demographic stochasticity. We can neglect this possibility
388 because the timescale of stochastic extinction from abundances of the order of n is much larger
389 than those of the processes under consideration.

390 5.2 Introduction of the variant by mutation (step 1)

391 As indicated above, we use a time-inhomogeneous Poisson point process to model the influx of
392 new mutations. The per capita rate of mutation is assumed to be constant through time but
393 whether or not a mutant will escape extinction within a host may depend on the type of host.
394 Indeed, a vaccine-escape mutation may have a higher probability to escape within-host extinction in
395 vaccinated hosts. We account for this effect by making a distinction between θ_U and θ_V . If vaccine-
396 escape mutations are more likely to escape extinction in vaccinated hosts we expect $\theta_V > \theta_U$. In
397 other words, $\theta_V/\theta_U - 1$ is a measure of the within-host fitness advantage of the vaccine-escape
398 mutant in vaccinated hosts (they are assumed to have the same within-host fitness in naïve hosts).

399 We can compute the probability that some of the vaccine-escape mutations are present as
400 standing variation before the start of vaccination. When the resident population has reached its
401 endemic equilibrium $(S_U^0, 0, I_{U,w}^0, 0, N^0)$, the number of mutants is approximated by a birth-and-
402 death process with immigration, with birth rate $b_m^0 = \beta_m \frac{S_U^0}{N^0}$ and death rate $d_m = \delta + \alpha_m + \gamma_m$,
403 and the “immigration” is actually mutations arising in the resident population, which occur at rate

404 $\mu_m = \theta_U I_{Uw}^0$. Because we assume that in a fully naïve host population vaccine-escape mutations
405 carry a fitness cost relative to the resident strain, we have $b_m^0 < d_m$. The number of mutants
406 thus approximately follows a subcritical birth-and-death process with immigration, which is known
407 to converge in distribution as $t \rightarrow \infty$ to a negative binomial stationary distribution [30]. The
408 probability that there are k infected individuals hosting the mutant pathogen at time $t = 0$ is thus:

$$p_k = \binom{k+r-1}{k} (1-R_m^0)^r (R_m^0)^k \quad (14)$$

409 where $r = \mu_m/b_m^0$ and $R_m^0 = b_m^0/d_m$. Hence the the expected number of vaccine-escape mutants
410 already present at the start of vaccination is

$$\frac{\mu_m}{d_m - b_m^0}. \quad (15)$$

411 This result is analogous to the classical result that the expected frequency of deleterious mutations
412 is of the form μ/s where μ is the rate of mutation towards deleterious mutants and s is the fitness
413 cost of those deleterious mutants.

414 We can also compute the probability that no mutant is present at the start of vaccination:

$$p_0 = (1 - R_m^0)^r \quad (16)$$

415 When either R_m^0 or r is small, $p_0 \approx 1$, and we can neglect the presence of preexisting mutants.
416 Otherwise, we need to account for the possibility that one or more mutants are present at time
417 $t = 0$, which we discuss in Section 5.5 below.

418 We now assume that there is zero mutant present at the start of vaccination. We are interested
419 in the law of the first time t_m at which a mutant appears. Because $\theta_U I_{Uw}(t) + \theta_V I_{Vw}(t)$ is the flux
420 of vaccine-escape mutants from the wild-type population, by the exponential formula for Poisson
421 point processes, we have [27]:

$$\mathbb{P}\{t_m > t\} = e^{-\int_0^t (\theta_U I_{Uw}(s) + \theta_V I_{Vw}(s)) ds}. \quad (17)$$

422 We can numerically compute the probability density function f_m of the first arrival time t_m of a
423 vaccine-escape mutant using

$$f_m(t) = \dot{F}_m(t)e^{-F_m(t)}, \quad (18)$$

424 where $F_m(t)$ is given by the auxiliary equation

$$\dot{F}_m = \theta_U I_{Uw}(t) + \theta_V I_{Vw}(t) \quad (19)$$

425 with initial condition $F_m(0) = 0$, while we compute $I_{Uw}(t)$ and $I_{Vw}(t)$ using (12). The use of this
426 auxiliary equation reduces computational effort by obtaining $F_m(t)$ simultaneously with $I_{Uw}(t)$ and
427 $I_{Vw}(t)$ (as opposed to computing the latter and then integrating).

428 5.3 Invasion of the variant (step 2)

429 Suppose that a mutant strain appears at time $t_m \geq 0$ in a single infected host, that is, with density
430 $I_m(0) = \frac{1}{n}$, (which is effectively zero as n becomes large). Then, (2) yields $I_m(t_m) \equiv 0$ for all t ,
431 whereas the dynamics of the system follows (12). This differential equation approximation does
432 not mean that the mutant is absent, but simply not sufficient in numbers to be visible at the coarse
433 resolution and short time scale upon which (12) is applicable.

434 Then we combine (12) with a birth-and-death process approximation, $\tilde{I}_m(t)$, to the *number*
435 of individuals infected with the mutant strain at time t after the mutant arrival time t_m , $I_m^n(t)$.
436 We approximate the rate of new infections, $\frac{\beta_m(S_U^n(t) + e_m S_V^n(t))}{N^n(t)}$ by replacing the stochastic quantities
437 $S_U^n(t)$, $S_V^n(t)$ and $N^n(t)$ by their deterministic approximations, giving the time-dependent birth
438 rate

$$b_m(t) = \frac{\beta_m(S_U(t) + e_m S_V(t))}{N(t)}$$

439 where $S_U(t)$, $S_V(t)$ and $N(t)$ are determined via the deterministic system (12). Each death in the
440 birth-and-death process corresponds to the removal of a susceptible, which occurs by host death or
441 recovery at combined rate $d_m = \delta + \alpha_m + \gamma_m$. See §8.2 in the Supplementary Information of [36]
442 for a rigorous justification.

443 The so-called “merciless dichotomy” [23] tells us that the time-inhomogeneous birth-and-death

444 process started with one individual at time t_m either goes extinct, or grows without bound (i.e.
 445 invades) with probability (see [24] and SI, Section 2)

$$P_m^{t_m} = \frac{1}{1 + \int_{t_m}^{\infty} d_m e^{-\int_{t_m}^t b_m(s) - d_m ds} dt}$$

446 Thus, either the mutant strain vanishes, or the number infected with the mutant strain will even-
 447 tually be of the order of n individuals, after which we can use (1) to compute the densities of both
 448 wild-type and mutant strains.

In practice, we can compute the probability of mutant invasion when the mutant is introduced at time t_m using $P_m^{t_m} = U_m^{t_m}(\infty)$ where $U_m^{t_m}(\infty)$ is obtained via the pair of auxiliary functions $U_m^{t_m}$ and $V_m^{t_m}$ [24] defined as follows: $U_m^{t_m}(t) = \mathbb{P}\{\tilde{I}_m(t) \neq 0\}$ and $V_m^{t_m}(t) = \mathbb{P}\{\tilde{I}_m(t) = 1 \mid \tilde{I}_m(t) \neq 0\}$, We then have

$$\dot{U}_m^{t_m} = -d_m U_m^{t_m} V_m^{t_m} \tag{20}$$

$$\dot{V}_m^{t_m} = (d_m - b_m(t)) V_m^{t_m} - d_m (V_m^{t_m})^2, \tag{21}$$

449 where $U_m^{t_m}(t_m) = V_m^{t_m}(t_m) = 1$ and we compute $b_m(t)$, $S_U(t)$, $S_V(t)$ and $N(t)$, via (12). In practice,
 450 we cannot compute $U_m^{t_m}(\infty)$; to obtain an approximation we evaluate $U_m^{t_m}(t)$ for sufficiently large
 451 t that $|U_m^{t_m}(t + \Delta t) - U_m^{t_m}(t)|$ is less than our desired threshold of error.

452 Note that several variants can arise and fail to invade before finally a lucky variant manages to
 453 invade. We can use the probability of invasion P_m^t of a variant introduced at time t to characterize
 454 the distribution of the first time t_i at which a mutant is introduced that successfully invades. By
 455 the thinning property of Poisson point processes, we have [27]:

$$\mathbb{P}\{t_i > t\} = e^{-\int_0^t (\theta_U I_{U_w}(s) + \theta_V I_{V_w}(s)) P_m^s ds} \tag{22}$$

456 where $\theta_U I_{U_w}(t) + \theta_V I_{V_w}(t)$ is the flux of vaccine-escape mutants from the wild-type population.
 457 We compute numerically the probability density function g_m of the first arrival time t_i of a vaccine-

458 escape mutant that successfully invades using

$$g_m(t) = \dot{G}_m(t)e^{-G_m(t)}, \quad (23)$$

459 where $G_m(t)$ is given by the auxiliary equation

$$\dot{G}_m(t) = (\theta_U I_{U_w}(t) + \theta_V I_{V_w}(t)) P_m^t \quad (24)$$

460 with initial condition $G_m(0) = 0$ and computing $I_{U_w}(t)$ and $I_{V_w}(t)$ using (12).

Compare (22) with (17) and note that the probability that no vaccine-escape mutant will ever *arise* is

$$\mathbb{P}\{t_m = \infty\} = e^{-\int_0^\infty (\theta_U I_{U_w}(t) + \theta_V I_{V_w}(t)) P_m^t dt}.$$

In contrast, the probability that no vaccine-escape mutant will ever *invade* is the larger probability

$$\mathbb{P}\{t_i = \infty\} = e^{-\int_0^\infty (\theta_U I_{U_w}(t) + \theta_V I_{V_w}(t)) P_m^t dt}.$$

Note that P_m^t converges as $t \rightarrow \infty$ to $P_m^* = 1 - 1/R_m^*$ which is nonzero, so that

$$\mathbb{P}\{t_m = \infty\} = 0 \Leftrightarrow \int_0^\infty (\theta_U I_{U_w}(t) + \theta_V I_{V_w}(t)) dt = \infty \Leftrightarrow \mathbb{P}\{t_i = \infty\} = 0,$$

461 that is, the probability of adaptation is 1 if and only if $t \mapsto (\theta_U I_{U_w}(t) + \theta_V I_{V_w}(t))$ is not integrable.

462 In other words, the probability of adaptation is 1 in the limit $t \rightarrow \infty$ when the wild type is not

463 driven to extinction by vaccination (i.e. $\nu < \nu_c$) which implies that there is an uninterrupted flux of

464 mutation producing vaccine-escape variants. One of these mutants will eventually escape extinction

465 and invade. Yet, the time needed for a successful variant to appear may be very long and we focus

466 in the main text on A_m^t the probability of adaptation before time t (equation (10) and Figure 6).

467 5.4 Fixation of the variant (step 3)

468 Suppose now that the mutant strain successfully invades; we next consider the probability P_{fix}
 469 that the mutant will outcompete the wild type and go to fixation. Fixation of the mutant occurs if
 470 it is still present when the wild-type strain disappears. If we let T_m and T_w be the extinction times
 471 of mutant and wild-type strains, the probability of mutant fixation is thus $\mathbb{P}\{T_w < T_m\}$ which we
 472 may decompose as

$$\begin{aligned} \int_{t_m}^{\infty} \mathbb{P}\{T_m > t\} \mathbb{P}\{T_w \in dt\} &= - \int_{t_m}^{\infty} \mathbb{P}\{T_m > t\} \frac{d}{dt} \mathbb{P}\{T_w > t\} dt \\ &= - \int_{t_m}^{\infty} \mathbb{P}\{I_m^n(t) > 0\} \frac{d}{dt} (1 - \mathbb{P}\{I_w^n(t) = 0\}) dt \quad (25) \\ &= \int_{t_m}^{\infty} \mathbb{P}\{I_m^n(t) > 0\} \frac{d}{dt} \mathbb{P}\{I_w^n(t) = 0\} dt. \end{aligned}$$

473 We again obtain estimates of $\mathbb{P}\{I_w^n(t) > 0\}$ and $\mathbb{P}\{I_m^n(t) > 0\}$ using the fact that conditional
 474 on $S_U(t)$, $S_V(t)$ and $N(t)$, $(\tilde{I}_w(t), \tilde{I}_m(t))$ follows a time-inhomogeneous, two-type birth-and-death
 475 process, where the birth rates for the two types, $i = w, m$, are given by

$$b_i(t) = \frac{\beta_i(S_U(t) + e_i S_V(t))}{N(t)}$$

476 and the death rates are $d_i = \delta + \alpha_i + \gamma_i$. The birth rates vary with time due to the epidemiological
 477 perturbations following the start of vaccination and in particular, to the feedback of mutant invasion
 478 on S_V and S_U . To quantify these epidemiological perturbations, we now approximate the density
 479 of susceptibles and total host density by the values of $S_U(t)$, $S_V(t)$ and $N(t)$ obtained from the full
 480 deterministic system (1), which accounts for the presence of the mutant by replacing I_m with its
 481 *expected value*.

482 We need to take care in choosing the initial conditions of (1) to account for the fact that we
 483 consider the time of appearance of the first mutant that successfully invades and so are conditioning
 484 on the non-extinction of the mutant strain, and for the inherent variability in the time required to
 485 invade; this results in a random initial condition for the deterministic dynamics (see Supplementary
 486 Information §4 for details). In practice, we find that the randomness has negligible effect, but

487 we must still take the conditioning into account. To do so, we first use (12) to compute the
 488 epidemiological dynamics of the wild type before the introduction of the mutant at time t_m . Then,
 489 at time t_m , we use (1) where $S_U(t_m)$, $S_V(t_m)$, $N(t_m)$ and $I_w(t_m)$ are obtained from (12) and take
 490 $I_m(t_m) = \frac{1}{(1-P_m^{t_m})^n}$ (see Supplementary Information §4). Crucially, the initial density of the mutant
 491 depends on the probability of successful invasion of the mutant $P_m^{t_m}$ obtained above.

492 Provided we use (1) with the appropriate initial conditions as previously, the birth rates of both
 493 the wild-type and mutant strains are approximately deterministic, and from [24], we have:

$$\mathbb{P}\{I_i^n(t) > 0\} \approx \mathbb{P}\{\tilde{I}_i(t) > 0\} = 1 - (1 - U_i^{t_m}(t))^{I_i^n(t_m)}, \quad (26)$$

494 where

$$U_i^{t_m}(t) = \frac{1}{1 + \int_{t_m}^t d_i e^{-\int_{t_m}^u b_i(s) - d_i ds} du} \quad (27)$$

495 is the probability that an individual infected with strain i ($i = m, w$) present at t_m has descendants
 496 alive at time t . Under the branching assumption, the lines of descent of distinct infected individuals
 497 are independent, hence the probability that strain i vanishes by time t is the product of the
 498 probabilities that each line of descent vanishes, $(1 - U_i^{t_m}(t))^{I_i^n(t_m)}$.

In practice, we need two pairs of auxiliary equations to track the probability of extinction of
 both the wild type and the mutant

$$\dot{U}_w^{t_m} = -d_w U_w^{t_m} V_w^{t_m} \quad (28)$$

$$\dot{V}_w^{t_m} = (d_w - b_w(t)) V_w^{t_m} - d_w (V_w^{t_m})^2 \quad (29)$$

$$\dot{U}_m^{t_m} = -d_m U_m^{t_m} V_m^{t_m} \quad (30)$$

$$\dot{V}_m^{t_m} = (d_m - b_m(t)) V_m^{t_m} - d_m (V_m^{t_m})^2, \quad (31)$$

499 with $U_w^{t_m}(t_m) = V_w^{t_m}(t_m) = U_m^{t_m}(t_m) = V_m^{t_m}(t_m) = 1$. To compute the probability of fixation, we
 500 first consider the probability of fixation prior to time t , which is derived in exactly the same manner
 501 as (25).

$$U^{t_m}(t) = \int_{t_m}^t \mathbb{P}\{I_m^n(s) > 0\} \frac{d}{dt} \mathbb{P}\{I_w^n(s) = 0\} ds,$$

502 Using (26) to approximate the probabilities $\mathbb{P}\{I_m^n(s) > 0\}$ and $\mathbb{P}\{I_w^n(s) = 0\}$, we get

$$U^{t_m}(t) = \int_{t_m}^t [1 - (1 - U_m^{t_m}(s))^{I_m^n(t_m)}][I_w^n(t_m)(-\dot{U}_w^{t_m})(1 - U_w^{t_m}(s))^{I_w^n(t_m)-1}]ds.$$

503 Differentiating this and taking $I_w^n(t_m) = nI_w(t_m)$ and $I_m^n(t_m) = 1$ yields the following auxiliary
504 equation for $U^{t_m}(t)$:

$$\dot{U}^{t_m} = nI_w(t_m)(\delta + \alpha_w + \gamma_w)U_w^{t_m}V_w^{t_m}(1 - U_w^{t_m})^{nI_w(t_m)-1}U_m^{t_m}, \quad (32)$$

505 with initial condition $U^{t_m}(t_m) = 0$. We estimate the fixation probability as $P_{fix}^{t_m} = U^{t_m}(\infty)$ as
506 above.

507 5.5 Invasion and Fixation with Standing Variation

508 We now come back to the probability of adaptation from standing variation at time $t = 0$, using the
509 probability p_k that there are k mutants present at time $t = 0$ and the estimates for the probabilities
510 of invasion and fixation $P_m^{t_m}$ and $P_{fix}^{t_m}$, of a single mutant arriving at time t_m , taking $t_m = 0$. Recall
511 that p_k is negative binomial with success probability $R_m^0 = b_m^0/d_m$ and $r = \mu_m/b_m^0$ failures. Under
512 the branching process approximation, the chain of infections started by each mutation will go
513 extinct independently with probability $1 - P_m^0$. The probability of invasion is then the probability
514 that at least one line survives, $1 - (1 - P_m^0)^k$. Summing this over all possible values of k gives us
515 the invasion probability from standing variation,

$$\sum_{k=1}^{\infty} p_k (1 - (1 - P_m^0)^k) = 1 - p_0 - \sum_{k=1}^{\infty} p_k (1 - P_m^0)^k = 1 - \sum_{k=0}^{\infty} p_k (1 - P_m^0)^k.$$

516 Recalling that the probability generating function for the number of mutants at time $t = 0$ is

$$\sum_{k=0}^{\infty} p_k z^k = \left(\frac{1 - R_m^0}{1 - R_m^0 z} \right)^r,$$

517 which converges provided $|z| < \frac{1}{R_m^0}$, we see that the probability of invasion from standard variation
518 is $1 - \left(\frac{1 - R_m^0}{1 - R_m^0(1 - P_m^0)} \right)^r$.

Similarly, if there are k mutations at time $t = 0$, (26) gives us that $\mathbb{P}\{I_m^n(t) > 0 | I_m(0) = k\} \approx 1 - (1 - U_m^0(t))^k$, so proceeding as above, we find that the probability that the mutant is still present at time t , assuming that at least one individual was present at time $t = 0$ is approximately $1 - \left(\frac{1 - R_m^0}{1 - R_m^0(1 - U_m^0(t))}\right)^r$. Substituting this for $\mathbb{P}\{I_m^n(t) > 0\}$ in (25) and differentiating as above gives us an auxiliary equation analogous to (32) for $U^0(t)$, the probability that the mutant fixes starting from standing variation:

$$\begin{aligned}\dot{U}^0 &= \mathbb{P}\{I_m^n(s) > 0\} \frac{d}{dt} \mathbb{P}\{I_w^n(s) = 0\} \\ &= nI_w(0)(\delta + \alpha_w + \gamma_w)U_w^0V_w^0(1 - U_w^0)^{nI_w(0)-1} \left(1 - \left(\frac{1 - R_m^0}{1 - R_m^0(1 - U_m^0)}\right)^r\right).\end{aligned}$$

519 As previously, we obtain $P_{fix}^0 = \dot{U}^0(\infty)$ by choosing t sufficiently large that $\dot{U}^0(t)$ equilibrates.

520 5.6 Stochastic simulations

521 We carried out stochastic simulations to check the validity of our results (see **Figure S1**). We used
522 an individual-based simulation program for the Markov process described in **Table S1**. We start
523 the simulation when the system is at its endemic equilibrium before vaccination given by equation
524 (11) in section 5.1. Then we introduce a single host infected with the mutant pathogen at a time
525 t_m after the start of vaccination and we let the simulation run until one of the pathogen variants
526 (the wild-type or the mutant) goes extinct. If the wild-type goes extinct first we record this run as
527 a “mutant fixation event”. We ran 1000 replicates for each set of parameters and **Figure S1** plots
528 the proportion of runs that led to mutant fixation. Simulation code is available upon request and
529 will be deposited on zenodo after acceptance of the manuscript.

530

531 **Acknowledgements:** SG acknowledges support from the CNRS PEPS 2022 grant “VaxDurable”.

532 References

533 [1] Helen K Alexander and Sebastian Bonhoeffer. Pre-existence and emergence of drug resistance
534 in a generalized model of intra-host viral dynamics. *Epidemics*, 4(4):187–202, 2012.

- 535 [2] Helen K Alexander, Guillaume Martin, Oliver Y Martin, and Sebastian Bonhoeffer. Evo-
536 lutionary rescue: linking theory for conservation and medicine. *Evolutionary applications*,
537 7(10):1161–1179, 2014.
- 538 [3] H. Andersson and T. Britton. *Stochastic Epidemic Models and their Statistical Analysis*,
539 volume 151 of *Lecture notes in statistics*. Springer, New York, 2000.
- 540 [4] Graham Bell. Evolutionary rescue. *Annual Review of Ecology, Evolution, and Systematics*,
541 48:605–627, 2017.
- 542 [5] Yuhua Cai and Stefan A. H. Geritz. Resident-invader dynamics of similar strategies in fluctu-
543 ating environments. 2020.
- 544 [6] Philippe Carmona and Sylvain Gandon. Winter is coming: Pathogen emergence in seasonal
545 environments. *PLoS computational biology*, 16(7):e1007954, 2020.
- 546 [7] H el ene Chabas, S ebastien Lion, Antoine Nicot, Sean Meaden, Stineke van Houte, Sylvain
547 Moineau, Lindi M Wahl, Edze R Westra, and Sylvain Gandon. Evolutionary emergence of
548 infectious diseases in heterogeneous host populations. *PLoS biology*, 16(9):e2006738, 2018.
- 549 [8] Sarah Cobey, Daniel B Larremore, Yonatan H Grad, and Marc Lipsitch. Concerns about
550 sars-cov-2 evolution should not hold back efforts to expand vaccination. *Nature Reviews Im-*
551 *munology*, pages 1–6, 2021.
- 552 [9] Nicholas G Davies, Sam Abbott, Rosanna C Barnard, Christopher I Jarvis, Adam J Kucharski,
553 James D Munday, Carl AB Pearson, Timothy W Russell, Damien C Tully, Alex D Washburne,
554 et al. Estimated transmissibility and impact of sars-cov-2 lineage b. 1.1. 7 in england. *Science*,
555 372(6538), 2021.
- 556 [10] Troy Day, David A Kennedy, Andrew F Read, and Sylvain Gandon. The evolutionary epidemi-
557 ology of pathogens during vaccination campaigns. *arXiv preprint arXiv:2109.13680*, 2021.
- 558 [11] Troy Day and Andrew F Read. Does high-dose antimicrobial chemotherapy prevent the evo-
559 lution of resistance? *PLoS computational biology*, 12(1):e1004689, 2016.

- 560 [12] Saad-Roy et al. Epidemiological and evolutionary considerations of sars-cov-2 vaccine dosing
561 regimes. *medRxiv*, 2020.
- 562 [13] S. Gandon and T. Day. The evolutionary epidemiology of vaccination. *J. Royal Soc. Interface*,
563 4(16):803–817, 2007.
- 564 [14] Sylvain Gandon and Troy Day. Evidences of parasite evolution after vaccination. *Vaccine*,
565 26:C4–C7, 2008.
- 566 [15] Sylvain Gandon and Sébastien Lion. Targeted vaccination and the speed of sars-cov-2 adap-
567 tation. *medRxiv*, 2021.
- 568 [16] Sylvain Gandon, Margaret Mackinnon, Sean Nee, and Andrew Read. Imperfect vaccination:
569 some epidemiological and evolutionary consequences. *Proceedings of the Royal Society of Lon-*
570 *don. Series B: Biological Sciences*, 270(1520):1129–1136, 2003.
- 571 [17] S. A. H. Geritz. Resident-invader dynamics and the coexistence of similar strategies. *J. Math.*
572 *Biol.*, 50(1):67–82, 2005.
- 573 [18] Philip J Gerrish, Fernando Saldana, Benjamin Galeota-Sprung, Alexandre Colato, Erika E
574 Rodriguez, and Jorge X Velasco-Hernandez. How unequal vaccine distribution promotes the
575 evolution of vaccine escape. *Available at SSRN 3827009*, 2021.
- 576 [19] Bryan Grenfell, Nicole Mideo, Laura C Pollitt, Andrew F Read, David L Smith, Claire Stan-
577 dley, Nina Wale, Geoffrey Chi-Johnston, Ted Cohen, Troy Day, et al. The path of least
578 resistance: aggressive or moderate. 2014.
- 579 [20] Bryan T Grenfell, Oliver G Pybus, Julia R Gog, James LN Wood, Janet M Daly, Jenny A
580 Mumford, and Edward C Holmes. Unifying the epidemiological and evolutionary dynamics of
581 pathogens. *science*, 303(5656):327–332, 2004.
- 582 [21] Matthew Hartfield and Samuel Alizon. Within-host stochastic emergence dynamics of immune-
583 escape mutants. *PLoS computational biology*, 11(3):e1004149, 2015.

- 584 [22] Jan Humplik, Alison L Hill, and Martin A Nowak. Evolutionary dynamics of infectious diseases
585 in finite populations. *Journal of theoretical biology*, 360:149–162, 2014.
- 586 [23] P. Jagers. Stabilities and instabilities in population dynamics. *J. Appl. Prob.*, pages 770–780,
587 1992.
- 588 [24] D. G. Kendall. On the generalized “Birth-and-Death” process. *Ann. Math. Stat.*, 19(1):1–15,
589 1948.
- 590 [25] David A Kennedy and Andrew F Read. Why does drug resistance readily evolve but vaccine re-
591 sistance does not? *Proceedings of the Royal Society B: Biological Sciences*, 284(1851):20162562,
592 2017.
- 593 [26] David A Kennedy and Andrew F Read. Why the evolution of vaccine resistance is less of a
594 concern than the evolution of drug resistance. *Proceedings of the National Academy of Sciences*,
595 115(51):12878–12886, 2018.
- 596 [27] John Frank Charles Kingman. *Poisson processes*, volume 3. Clarendon Press, 1992.
- 597 [28] Oleg Kogan, Michael Khasin, Baruch Meerson, David Schneider, and Christopher R My-
598 ers. Two-strain competition in quasineutral stochastic disease dynamics. *Physical Review E*,
599 90(4):042149, 2014.
- 600 [29] T. G. Kurtz. *Approximation of Population Processes*, volume 36. Society for Industrial and
601 Applied Mathematics, Philadelphia, 1981.
- 602 [30] Amaury Lambert. Population dynamics and random genealogies. *Stochastic Models*,
603 24(sup1):45–163, 2008.
- 604 [31] Gabriela Lobinska, Ady Pazner, Arne Traulsen, Yitzhak Pilpel, and Martin A Nowak. Evo-
605 lution of resistance to covid-19 vaccination with dynamic social distancing. *Nature human*
606 *behaviour*, 6(2):193–206, 2022.
- 607 [32] Guillaume Martin, Robin Aguilée, Johan Ramsayer, Oliver Kaltz, and Ophélie Ronce. The
608 probability of evolutionary rescue: towards a quantitative comparison between theory and

- 609 evolution experiments. *Philosophical Transactions of the Royal Society B: Biological Sciences*,
610 368(1610):20120088, 2013.
- 611 [33] Hamish McCallum, Nigel Barlow, and Jim Hone. How should pathogen transmission be mod-
612 elled? *Trends in ecology & evolution*, 16(6):295–300, 2001.
- 613 [34] AngelaR McLean. After the honeymoon in measles control. *The Lancet*, 345(8945):272, 1995.
- 614 [35] David V McLeod, Lindi M Wahl, and Nicole Mideo. Mosaic vaccination: how distributing
615 different vaccines across a population could improve epidemic control. *bioRxiv*, pages 2020–11,
616 2021.
- 617 [36] T. L. Parsons, A. Lambert, T. Day, and S. Gandon. Pathogen evolution in finite populations:
618 slow and steady spreads the best. *J. Royal Soc. Interface*, 15(147), 2018.
- 619 [37] Robert S Paton, Christopher E Overton, and Thomas Ward. The rapid replacement of the
620 delta variant by omicron (b. 1.1. 529) in england. *Sci. Transl. Med.*, page eabo5395, 2022.
- 621 [38] Tadeas Priklopil and Laurent Lehmann. Invasion implies substitution in ecological communities
622 with class-structured populations. 134:36–52, 2020.
- 623 [39] Jason W Rausch, Adam A Capoferri, Mary Grace Katusiime, Sean C Patro, and Mary F
624 Kearney. Low genetic diversity may be an achilles heel of sars-cov-2. *Proceedings of the*
625 *National Academy of Sciences*, 117(40):24614–24616, 2020.
- 626 [40] Andrew F Read, Troy Day, and Silvie Huijben. The evolution of drug resistance and the curi-
627 ous orthodoxy of aggressive chemotherapy. *Proceedings of the National Academy of Sciences*,
628 108(Supplement 2):10871–10877, 2011.
- 629 [41] Simon A Rella, Yuliya A Kulikova, Emmanouil T Dermitzakis, and Fyodor A Kondrashov.
630 Rates of sars-cov-2 transmission and vaccination impact the fate of vaccine-resistant strains.
631 *Scientific Reports*, 11(1):1–10, 2021.
- 632 [42] Olivier Restif and Bryan T Grenfell. Vaccination and the dynamics of immune evasion. *Journal*
633 *of the Royal Society Interface*, 4(12):143–153, 2007.

- 634 [43] Rafael Sanjuán, Miguel R Nebot, Nicola Chirico, Louis M Mansky, and Robert Belshaw. Viral
635 mutation rates. *Journal of virology*, 84(19):9733–9748, 2010.
- 636 [44] Robin N Thompson, Edward M Hill, and Julia R Gog. Sars-cov-2 incidence and vaccine escape.
637 *The Lancet Infectious Diseases*, 2021.
- 638 [45] Stineke van Houte, Alice KE Ekroth, Jenny M Broniewski, Hélène Chabas, Ben Ashby, Joseph
639 Bondy-Denomy, Sylvain Gandon, Mike Boots, Steve Paterson, Angus Buckling, et al. The
640 diversity-generating benefits of a prokaryotic adaptive immune system. *Nature*, 532(7599):385–
641 388, 2016.
- 642 [46] Erik Volz, Swapnil Mishra, Meera Chand, Jeffrey C Barrett, Robert Johnson, Lily Geidelberg,
643 Wes R Hinsley, Daniel J Laydon, Gavin Dabrera, Áine O’Toole, et al. Assessing transmissibility
644 of sars-cov-2 lineage b. 1.1. 7 in england. *Nature*, 593(7858):266–269, 2021.
- 645 [47] Pengfei Wang, Manoj S Nair, Lihong Liu, Sho Iketani, Yang Luo, Yicheng Guo, Maple Wang,
646 Jian Yu, Baoshan Zhang, Peter D Kwong, et al. Antibody resistance of sars-cov-2 variants b.
647 1.351 and b. 1.1. 7. *Nature*, pages 1–6, 2021.

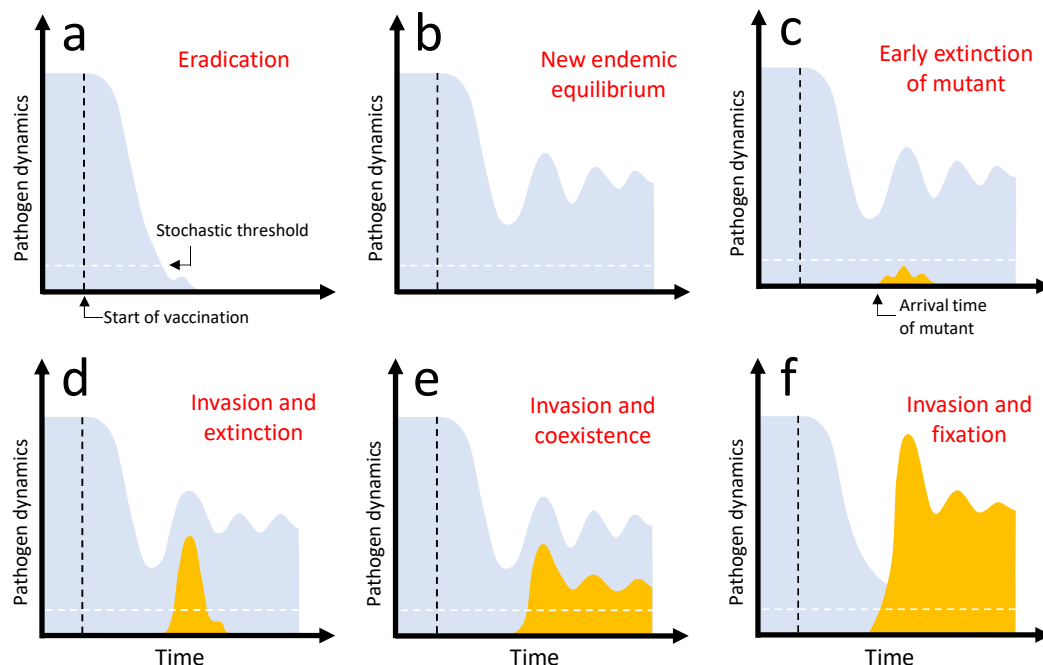


Figure 1: Graphical representation of the different evolutionary epidemiology outcomes after vaccination. The density of the wild-type pathogen is indicated in light blue and the dynamics of the mutant in orange. Each panel describes the temporal dynamics of the epidemics after the start of vaccination: (a) eradication of the wild-type pathogen, (b) new endemic equilibrium of the wild-type population after damped oscillations (with no introduction of the vaccine-adapted mutant), (c) early extinction of the vaccine-adapted mutant after its introduction by mutation, (d) invasion of the vaccine-adapted mutant followed by its extinction, (e) invasion of the vaccine-adapted mutant and long-term coexistence with the wild type in a new endemic equilibrium after damped oscillations, (f) invasion and fixation of the vaccine-adapted mutant (extinction of the wild type). Note that (b), (c) and (d) result to the same endemic equilibrium (wild-type population) after damped oscillations. The vertical dashed line (black) indicates the start of vaccination. For simplicity we consider that vaccination starts after the wild-type population has reached an endemic equilibrium. The horizontal dashed line indicates the “stochastic threshold” above which one may consider that the deterministic model provides a very good approximation of the dynamics and we can neglect the effect of demographic stochasticity.

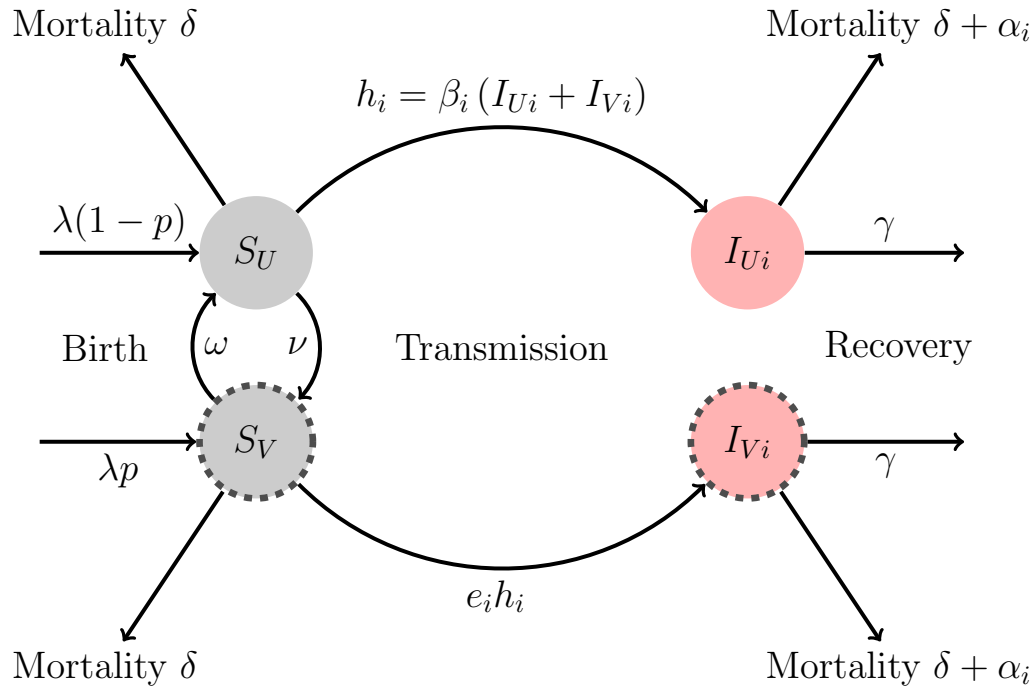


Figure 2: A schematic representation of the model. Naive and uninfected hosts (S_U hosts) are introduced at a rate λ and are vaccinated with probability p at birth and at rate ν later on. Immunization induced by the vaccine wanes at rate ω . Uninfected hosts (S_U and S_V) die at a rate δ while infected hosts (I_{U_i} and I_{V_i}) die at a rate $d_i = \delta + \alpha_i$, where i refers to the virus genotype: the wild-type ($i = w$) or the escape mutant ($i = m$). The rate of infection of naive hosts by the genotype i is $h_i = \beta_i(I_{U_i} + I_{V_i})$, where β_i is the transmission rate of the genotype i . Vaccination reduces the force of infection and e_i refers to the ability of the genotype i to escape the immunity triggered by vaccination (we assume $e_m > e_w$). A host infected by parasite genotype i recovers from the infection at rate γ_i and yields lifelong and perfect immunity (R hosts). $N = S_U + S_V + \sum_i(I_{U_i} + I_{V_i}) + R$ is the total host population density.

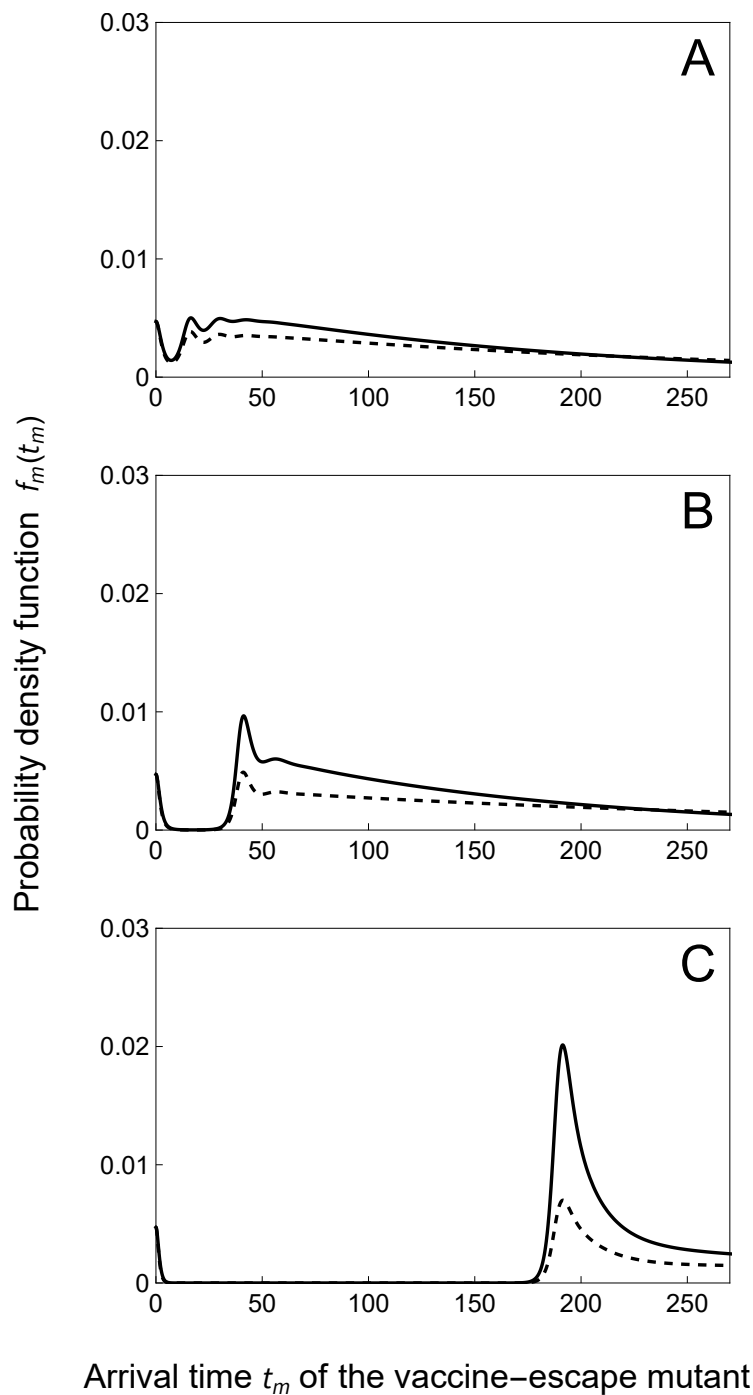


Figure 3: Faster vaccine rollout delays the arrival time of the mutant. We plot the probability density function $f_m(t)$ of the arrival time of the mutant for different speeds of vaccination rollout: $\nu = 0.1$ (top), 0.2 (middle) and 0.3 (bottom). We contrast a scenario where $\theta_V = \theta_U$ (dashed line), and $\theta_V = 10 \times \theta_U$ (full line). Other parameter values: $\theta_U = 1$, $\lambda = 0.01$, $\delta = 0.01$, $\gamma = 1$, $\beta_w = 20$, $\alpha_w = 1$, $e_w = 0.03$, $\omega = 0.05$, $p = 0.1$. For these parameter values the critical rate of vaccination ν_c above which the wild-type pathogen is driven to extinction is $\nu_c \approx 0.54$ (see equation (5)).

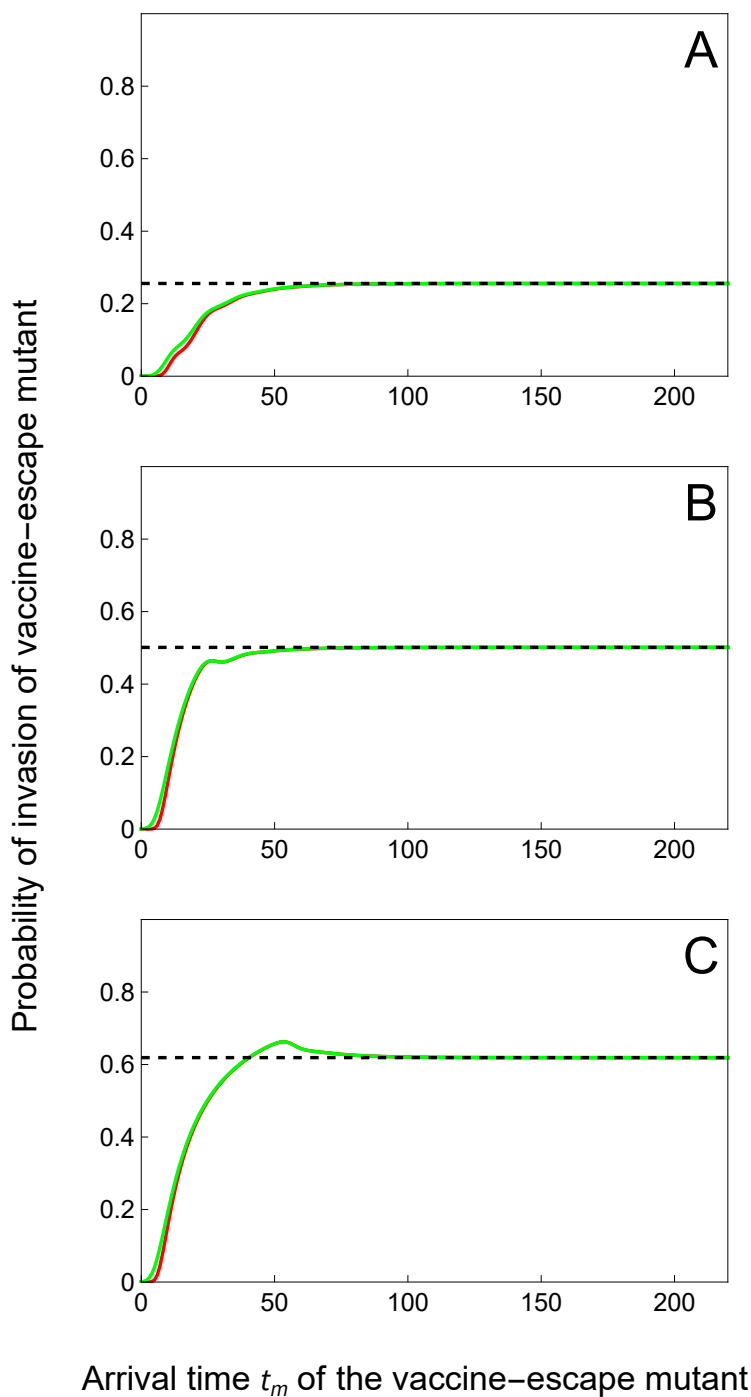


Figure 4: Probability of invasion of the vaccine-escape mutant increases with t_m . We plot the probability invasion $P_m^{t_m}$ of a slow (green) and a fast (red) vaccine-escape mutant for different speeds of vaccination rollout: $\nu = 0.1$ (top), 0.2 (middle) and 0.3 (bottom). The slow mutant: $e_m = 1, \beta_m = 10, \alpha_m = 1$. The fast mutant: $e_m = 1, \beta_m = 30, \alpha_m = 5.02$. The probability of invasion P_m^* in the limit $t_m \rightarrow \infty$ (see equation (9)) is indicated with the dashed black line. Other parameter values: $\lambda = 0.01, \delta = 0.01, \gamma = 1, \beta_w = 20, \alpha_w = 1, e_w = 0.03, \omega = 0.05, p = 0.1$.

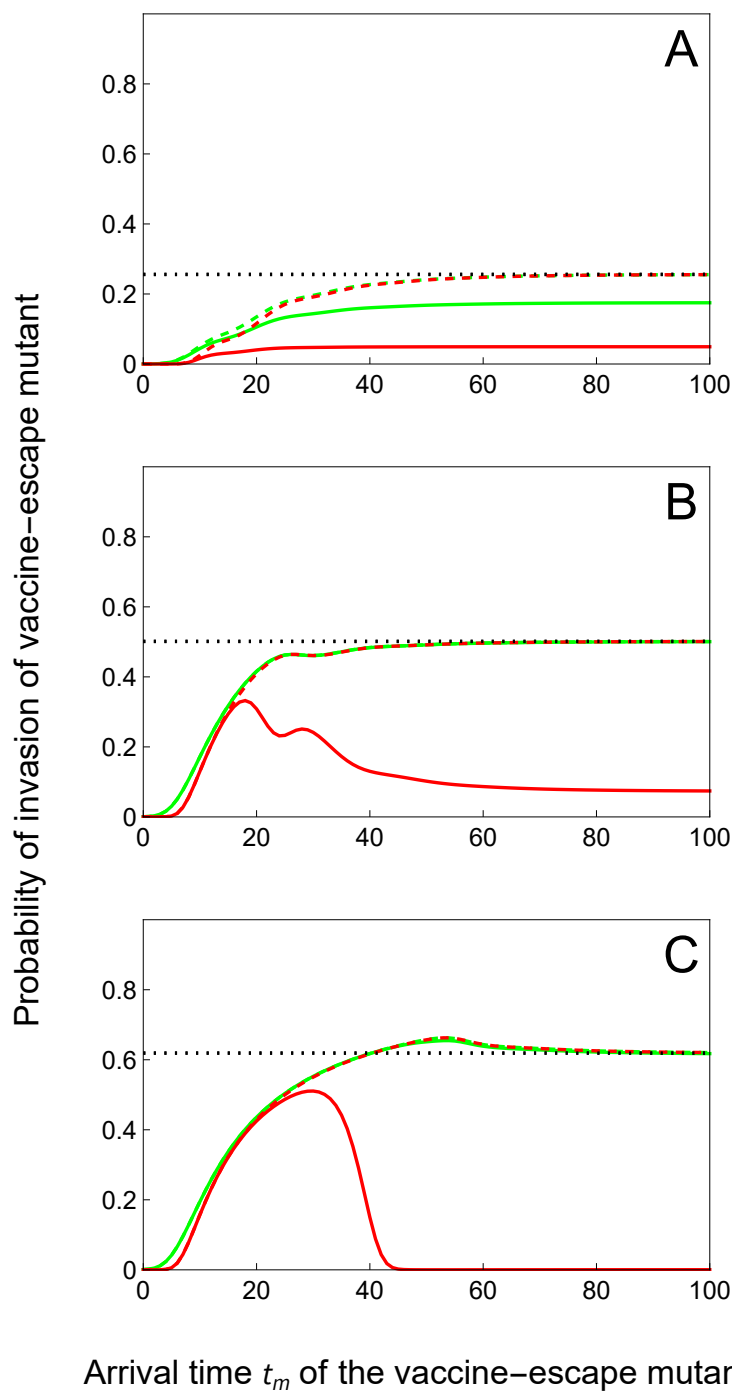


Figure 5: Probability of fixation of the vaccine-escape mutant may be low when t_m is large. We plot the probability of fixation of a slow (green) and a fast (red) vaccine-escape mutant for different speeds of vaccination rollout: $\nu = 0.1$ (top), 0.2 (middle) and 0.3 (bottom). The slow mutant: $e_m = 1, \beta_m = 10, \alpha_m = 1$. The fast mutant: $e_m = 1, \beta_m = 30, \alpha_m = 5.02$. For comparison with **Figure 4** we plot the probability of invasion $P_m^{t_m}$ with dashed colored lines and its asymptotic value P_m^* with a dashed black line. Other parameter values: $\lambda = 0.01, \delta = 0.01, \gamma = 1, \beta_w = 20, \alpha_w = 1, e_w = 0.03, \omega = 0.05, p = 0.1, n = 10^8$.

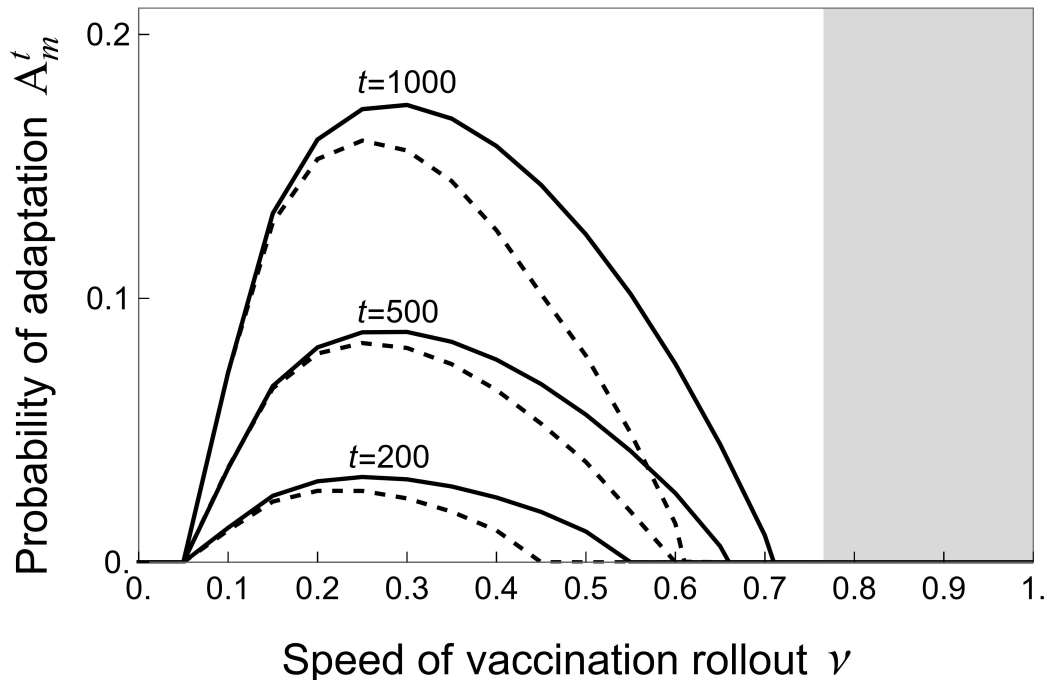


Figure 6: Probability of adaptation and the speed of vaccination rollout. We plot the probability of adaptation A_m^t of a vaccine-escape mutant against the speed of vaccination rollout for different values of time t (black line). The dashed line indicates the probability of adaptation when we impose periodic fluctuations in $c(t)$ which measures the intensity of Non-Pharmaceutical Interventions (NPIs) that reduce the transmission rate of all pathogens by $1 - c(t)$. Here we use a square wave function for $c(t)$ that fluctuates between 0.2 and 0 with a period $T = 200$. These NPIs affect both the flux of mutations (**Figure S3**) and the probability of invasion (**Figure S4**). The light gray area on the right-hand-side indicates the speed above which the wild-type pathogen is expected to be driven to extinction ($\nu > \nu_c$). In the absence of NPIs the critical rate of vaccination ν_c above which the wild-type pathogen is driven to extinction is $\nu_c \approx 0.77$ (see equation (5)). Parameter values: $\lambda = 0.01$, $\delta = 0.01$, $\gamma = 1$, $\beta_w = 20$, $\alpha_w = 1$, $e_w = 0.03$, $\beta_m = 10$, $\alpha_m = 1$, $e_m = 1$, $\omega = 0.05$, $p = 0$, $\theta_V = \theta_U = 0.1$.